Accepted Manuscript

Development of a Scalable Palladium-catalyzed α-Arylation Process for the Synthesis of a CGRP Antagonist

Lopa V. Desai, Michael Hay, David Leahy, Carolyn Wei, Dayne Fanfair, Thorsten Rosner, Yi Hsiao

PII: S0040-4020(13)00595-4

DOI: 10.1016/j.tet.2013.04.057

Reference: TET 24257

To appear in: *Tetrahedron*

Received Date: 2 March 2013

Revised Date: 12 April 2013

Accepted Date: 15 April 2013

Please cite this article as: Desai LV, Hay M, Leahy D, Wei C, Fanfair D, Rosner T, Hsiao Y, Development of a Scalable Palladium-catalyzed α-Arylation Process for the Synthesis of a CGRP Antagonist, *Tetrahedron* (2013), doi: 10.1016/j.tet.2013.04.057.

Development of a Scalable Palladium-catalyzed α-Arylation Process for the Synthesis of a CGRP Antagonist

Lopa V. Desai*, Michael Hay*, David K. Leahy, Carolyn Wei, Dayne Fanfair, Thorsten Rosner, Yi Hsiao

Corresponding authors' email addresses: lopa.desai@bms.com; michael.hay@bms.com

Corresponding authors' phone numbers: 732-227-5443; 732-227-6267

Corresponding authors' fax numbers: 732-227-3002

Chemical Development, Bristol-Myers Squibb, 1 Squibb Dr., New Brunswick, NJ 08903, USA

Graphical Abstract:

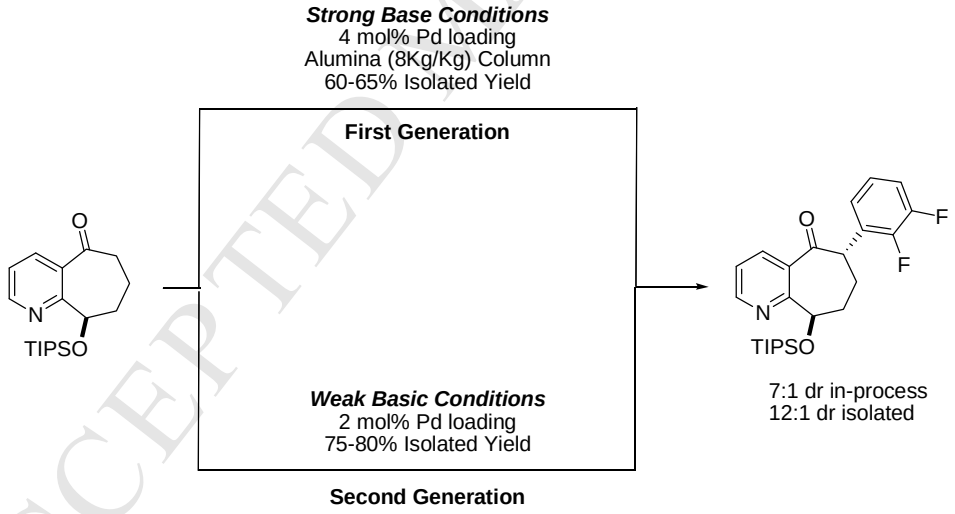

Development of a Scalable Palladium-catalyzed α-Arylation Process for the Synthesis of a CGRP Antagonist

Lopa V. Desai*, Michael Hay*, David Leahy, Carolyn Wei, Dayne Fanfair, Thorsten Rosner, Yi Hsiao

Chemical Development, Bristol-Myers Squibb, 1 Squibb Dr., New Brunswick, NJ 08903, USA

Corresponding authors' email addresses: lopa.desai@bms.com; michael.hay@bms.com

Corresponding authors' phone numbers: 732-227-5443; 732-227-6267

Corresponding authors' fax numbers: 732-227-3002

Key Words: Catalysis, α-Arylation, Palladium, heteroaromatic ketone

1. Abstract

The Pd-catalyzed α-arylation of cycloheptapyridyl ketone is a key complexity-building step in the synthesis of BMS-846372, a CGRP antagonist. A first generation process utilized $Pd(OAc)_2$/P*t*Bu_3.HBF_4 catalyst system with a strong base NaO*t*Bu. Although this process was demonstrated on multi-kilo scale, the harsh conditions led to non-selective metal catalyzed processes which generated several operational, quality and throughput issues. By acquiring detailed knowledge around several important process parameters, we were able to design an efficient and scalable second generation α-arylation process using a $Pd(OAc)_2$/RuPhos catalyst system with the weaker base, K_3PO_4 in t-amyl alcohol. This new weak base process was high yielding, efficient and superior in several respects compared to the strong base process. The strategy behind the reaction and isolation development and the process considerations important to scaling a catalytic reaction from laboratory to manufacturing scale will be discussed.

2. Introduction

Secretion of Calcitonin Gene Related Peptide (CGRP), a 37 amino acid neuropeptide, is known to increase during a migraine attack, leading to abnormal vascular activity of the intracranial arteries.[1] BMS-846372 is a potent CGRP antagonist with the potential to be effective in relieving migraines.[2] We envisioned synthesizing BMS-846372 from intermediates **1** and **2** using a palladium-catalyzed α-arylation reaction followed by reduction of the carbonyl group.[3] The α-arylation reaction is an attractive transformation for the rapid construction of C-C bonds alpha to a carbonyl moiety,[4] Miura,[5] Buchwald,[6] Hartwig[7] and others[8] have shown that this transformation is effective for the coupling of various aryl halides with esters, amides, aliphatic ketones, aldehydes and more recently heteroaromatic ketones.[9] Both electron deficient and rich aryl halides have been successfully employed, rendering the α-arylation reaction versatile and synthetically valuable[8a]. However, to the best of our knowledge, this transformation has not been applied on a manufacturing scale, even though this disconnection is strategically constructive. Herein, we present a diasteroeselective and scalable synthesis of advanced intermediate **3** through a palladium-catalyzed α-arylation reaction. We will provide a detailed discussion on the process considerations important to scaling a catalytic reaction from laboratory to manufacturing scale.

Figure 1: Retrosynthetic Strategy to Access BMS-846372

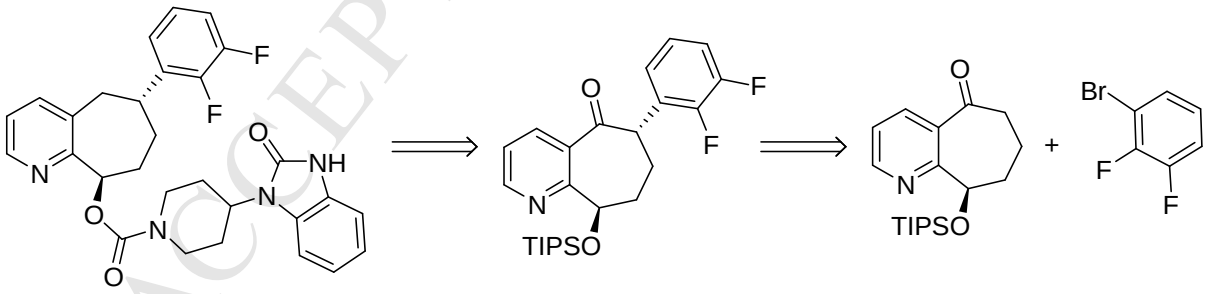

3. Results and Discussion

2.1 First Generation Development: Strong Base α-Arylation

Our initial reaction development began by screening ligands, bases, and catalysts in various solvents at 120 °C to effect the α-arylation reaction of **1** with aryl bromide **2**. Notably, the reaction afforded the product as a 6:1 thermodynamic ratio of diastereomers, whereby the major trans-diastereomer **3** was the desired product (Scheme 1). Due to tight timelines, we were not able to perform an extensive screen. From the few solvents that we screened, toluene was the most effective for the desired transformation. After screening various Pd(II) and Pd(0) pre-cursors, $Pd(OAc)_2$ and $Pd_2(dba)_3$ afforded the product in reasonable yield. As shown in Table 1, $Pd(OAc)_2$ was found to be the metal precursor of choice with all the ligands (e.g. entries 17 and 18), with Cs_2CO_3, K_3PO_4, and NaO*t*Bu as effective bases. Interestingly, other carbonate, phosphate and *tert*-butoxide bases (Na_2CO_3, K_2CO_3, Li_3PO_4, Na_3PO_4, LiO*t*Bu and KO*t*Bu) afforded <5% of the desired product suggesting a strong correlation between ligand and the base. A greater yield of product **3** was obtained when ligands S-Phos, MePhos and P*t*Bu$_3$·HBF$_4$ were used with NaO^{t}Bu as a base (Table 1, entries 9, 12 and 17).[10] From these results, we chose to focus our initial optimization and development work on the P*t*Bu$_3$·HBF$_4$/NaO*t*Bu conditions due to the ready availability of the phosphine ligand.

Table 1: Representative Screening Results[a]

Entry	Catalyst	Ligand	Base	Conversion (%)[b]
1	$Pd(OAc)_2$	S-Phos	Na_3PO_4	1%
2	Pd_2dba_3	DPEPhos	KO*t*Bu	16%
3	$Pd(OAc)_2$	CxPOMeCy	Cs_2CO_3	38%
4	$Pd(OAc)_2$	CxPOMeCy	K_3PO_4	50%
5	$Pd(OAc)_2$	XantPhos	K_3PO_4	5%
6	$Pd(OAc)_2$	XantPhos	Cs_2CO_3	14%
7	$Pd(OAc)_2$	Binap	Cs_2CO_3	19%
8	$Pd(OAc)_2$	S-Phos	Cs_2CO_3	27%
9	$Pd(OAc)_2$	S-Phos	NaOtBu	40%
10	Pd_2dba_3	MePhos	K_3PO_4	6%

11	Pd_2dba_3	MePhos	NaOtBu	45%
12	$Pd(OAc)_2$	MePhos	NaOtBu	50%
13	$Pd(OAc)_2$	$PtBu_3.HBF_4$	K_2CO_3	1%
14	$Pd(OAc)_2$	D^tBPF	K_3PO_4	2%
15	$Pd(OAc)_2$	D^tBPF	NaOtBu	44%
16	$Pd(OAc)_2$	$PtBu_3.HBF_4$	K_3PO_4	45%
17	$Pd(OAc)_2$	$PtBu_3.HBF_4$	NaO*t*Bu	50%
18	Pd_2dba_3	$PtBu_3.HBF_4$	NaO*t*Bu	40%

[a] Conditions: **1** (1 equiv), **2** (1.1 equiv), Base (1.3 equiv), Pd precursor (0.05 equiv Pd), monodentate ligand (0.1 equiv)/ bidentate ligand (0.05 equiv), base (2 equiv), toluene (10 ml/g **1**), 120 °C

[b] Conversion based on HPLC area percent of product and starting material

Scheme 1: Pd-catalyzed α-Arylation of 1 with Arylbromide 2

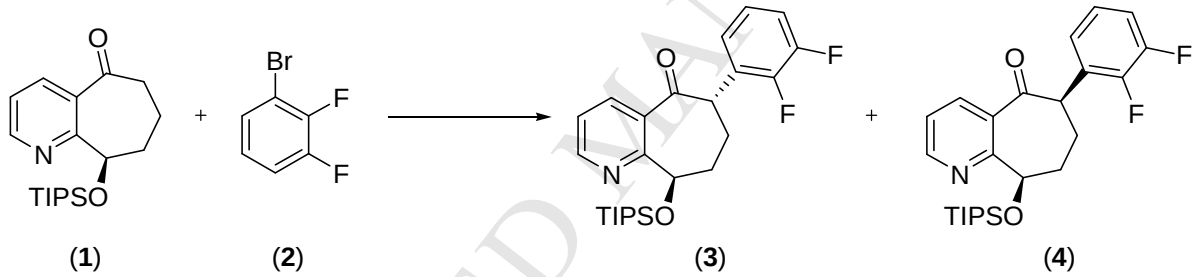

(**1**) (**2**) (**3**) (**4**)

Optimization of this lead result focused on examining the effect of concentration and temperature on the reaction kinetics and impurity profile. We observed a large discrepancy between the overall conversion and the solution yield of the product (Figure 2) resulting from the formation of several impurities (Figure 3), some of which were observed to be highly colored. After conducting several control experiments and understanding the origin and fate of some of the impurities we realized that majority of the impurities, including the highly colored ones, resulted from undesired base-induced decomposition of the starting material and the product. We reasoned that lowering the reaction temperature would slow down the rate of this decomposition. Indeed, lowering the reaction temperature to 95 °C slowed down the rate of decomposition, which addressed the discrepancy between conversion and yield, but did not entirely mitigate it. Our approach to mitigate this discrepancy began with careful consideration of each

reaction parameter. Under these conditions, the reaction is sensitive to a) ligand particle size, wherein finely powdered ligand improved the yield of **3**, b) moisture and c) oxygen content. Due to the instability of the product to the highly basic conditions, the base charge had to be within 1.3–1.5 equivalents and the reaction had to be cooled to 25 °C shortly after reaching completion in order to maximize the solution yield.

Figure 2: Reaction Profile of the α-Arylation Reaction at Different Concentrations and Temperatures

Conditions: **1** (1 equiv), **2** (1.1 equiv), NaOtBu (1.3 equiv), $Pd(OAc)_2$ (0.04 equiv), $PtBu_3.HBF_4$ (0.04 equiv), solvent (7 or 3 mL/g of **1**), 120 or 95 °C

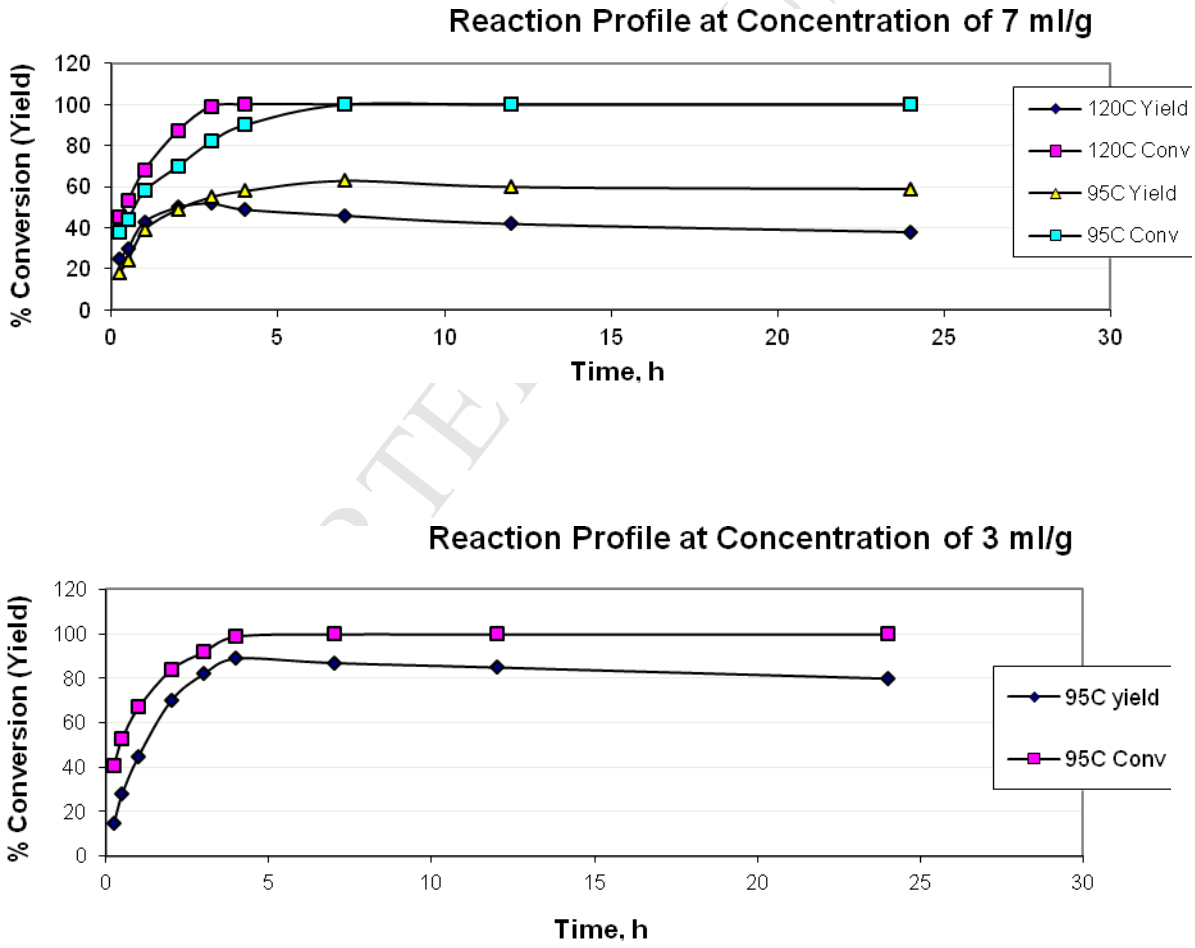

The major impurities observed for the P*t*Bu$_3$·HBF$_4$/NaO*t*Bu system were **5** and **6** (Figure 3).[11] We believe **6** is formed via the mechanism illustrated in Figure 4. Complex

11, formed from the reaction of enolate **10** with oxidative addition complex **9**, could undergo cyclopalladation with the aromatic C-H bond forming complex **13**.[12] Carbon-carbon bond forming reductive elimination followed by nucleophilic displacement of the fluoride by the enolate affords **6**. Based on the mechanism, we hypothesized that the ligand to metal ratio should have an effect on the formation of **6**. Excess ligand would occupy a coordination site on palladium in complex **11**/**12** and disfavor the agostic interaction with the aromatic C-H bond. We examined ligand:metal ratios from 1:1 to 3:1 and observed that higher ligand content reduced the level of **6** formed during the course of the reaction, although at the expense of reaction rate (Table 2).[13]

Figure 3: Impurities Formed During the α-Arylation Reaction

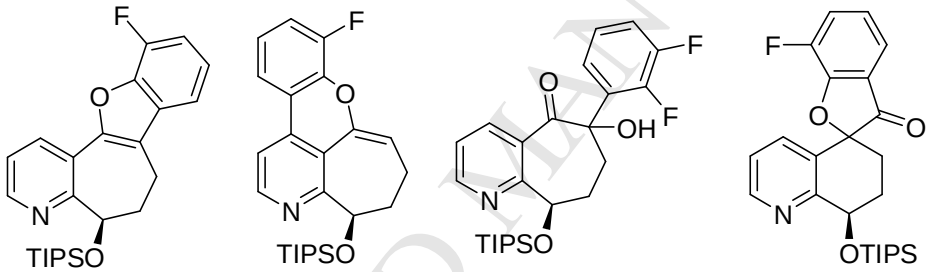

Figure 4: Proposed Mechanism for the Formation of Impurity 6

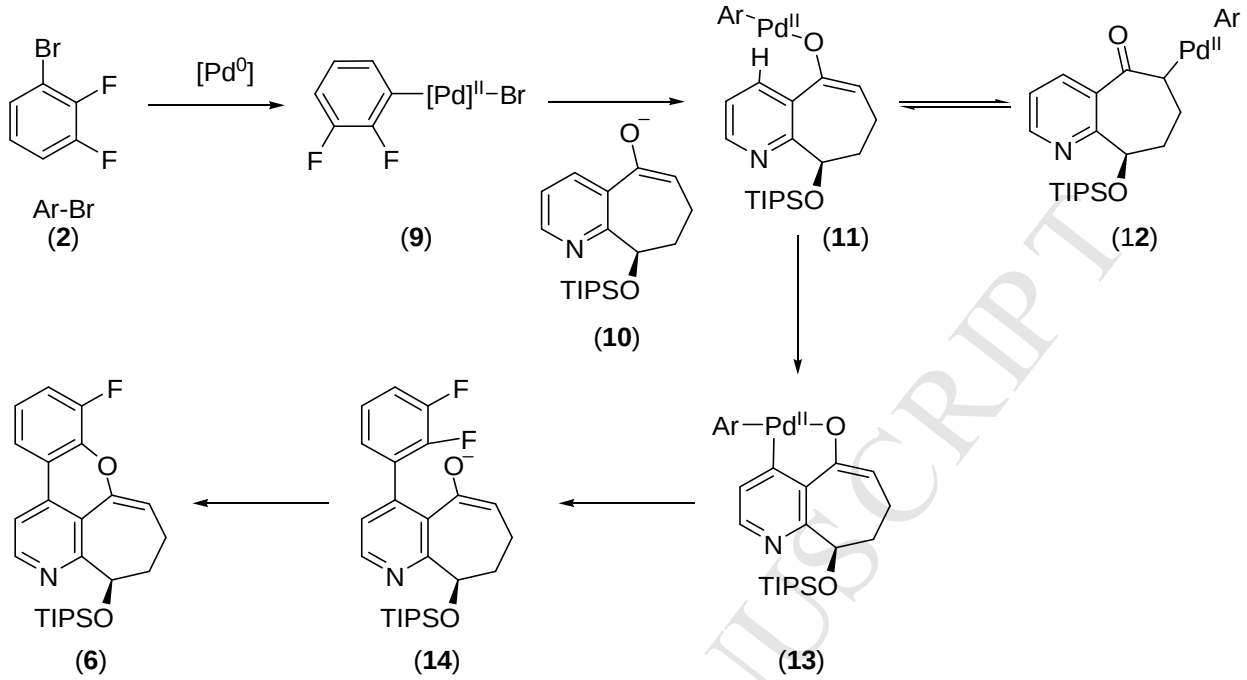

Table 2: Effect of L:M ratio on Reaction Performance and Formation of Impurity 6[a]

Entry	L:M	% Conversion	HPLC Area % of 6
1	0.9:1	96	2.1
2	1:1	91	1.6
3	2:1	95	0.3

[a] Conditions: **1** (1 equiv), **2** (1.1 equiv), NaO*t*Bu (1.3 equiv), $Pd(OAc)_2$ (0.04 equiv), $PtBu_3.HBF_4$, Toluene (4 ml/g **1**), 95 °C, 4 h

Other reaction impurities, including **5**, **7** and **8** are related to the reaction of starting material **1** or product **3** with NaO*t*Bu. Based on control experiments, we found that subjection of desired product **3** to NaO*t*Bu in toluene at 95 °C in the presence of atmospheric oxygen led to the formation of impurity **7**, which could undergo base promoted reaction to afford **8**, presumably via a pinacolone based rearrangement. In the absence of oxygen, heating **3** in the presence of NaO*t*Bu led to the formation of benzofuran **5** (Scheme 3).

Scheme 3: Un-catalyzed Reaction of Product Forming Impurities 5, 7 and 8

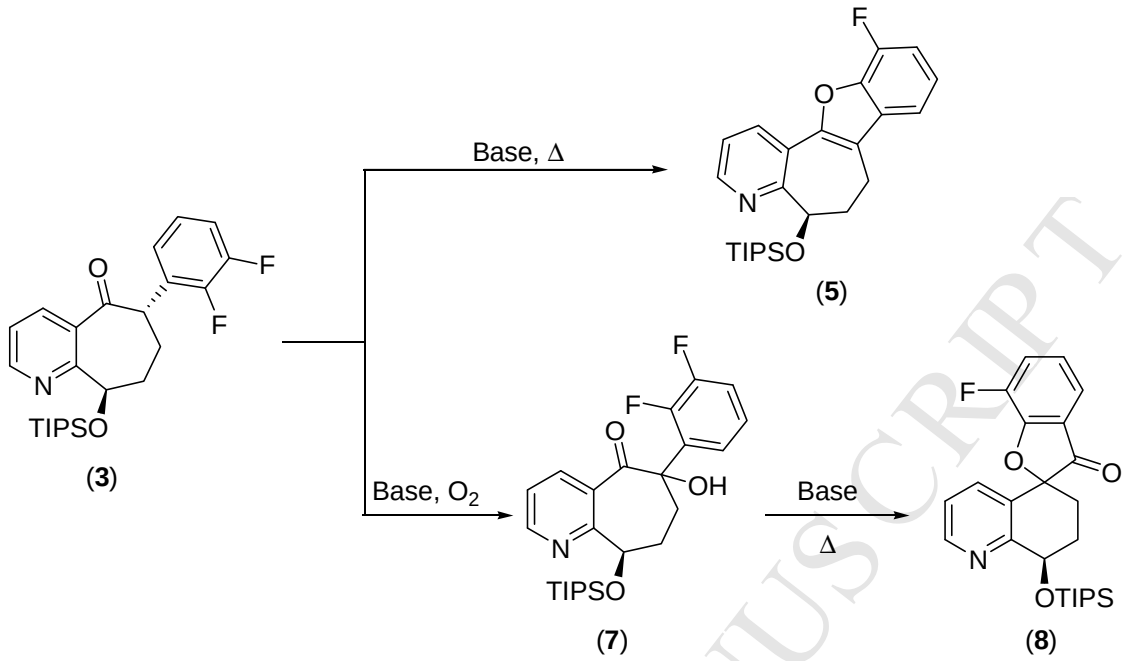

Based on this work, we employed the following optimized conditions: 4 mol% $Pd(OAc)_2$, 4 mol% P*t*Bu_3·HBF_4, 1.3 equiv NaO*t*Bu, 1.2 equiv ArBr (**2**) in toluene at 95 °C for 4 hours. These conditions afforded **3** in 82% solution yield as a 6:1 mixture of diastereomers (*trans*:*cis*). After performing the reaction on scale, we next needed to remove the metal, starting material and product related impurities. At the onset of our isolation development work, we observed that these impurities greatly impacted crystallization performance and thus several methods for removing them were explored. We initially examined carbon treatments, filtration through derivatized and underivatized silica gels, and resins. These treatments afforded streams that contained impurities **6**, **5**, and other unidentified impurities which a) increased the propensity for oiling during the crystallization, b) adversely affect the performance of downstream chemistry and c) resulted in isolated material that was colored and of poor quality. We found that washing the reaction stream with saturated aqueous NH_4Cl followed by filtration through activated alumina, constructed from 8 kg of alumina per kg of **1**, using 20 L/kg **1** of toluene, successfully removed these unidentified colored impurities and provided adequate crystallization performance i.e. affording solutions with 97% potency and 98% HPLC area purity.

Upon achieving acceptable quality of the post reaction stream, a controlled seeded crystallization protocol was developed using IPA/water (1:1 v/v). This procedure resulted in isolation of the product in 65-67% yield (98 wt% potency) with mother liquor losses of ~ 12 M%. Notably, the diastereomeric ratio of the isolated product increased from 6:1 to 10:1 *trans*:*cis*. We demonstrated the crystallization on 62 kg, 85 kg and 95 kg scale providing **3** in 61% average yield and 97.4% average HPLC area % purity (Table 3). The decrease in the yield of **3** is due to the level of **6**, batch 2, Table 3. It was difficult to control impurity **6** at a specific level or explain the variability in its levels between batches. Inconsistency in the performance of the alumina column resulted in poor quality and purity of **3**, batch 3, Table 3.

Table 3: Pilot Plant Batches with Strong Base α-Arylation Process[a]

Batch	1 (kg)	3 (kg)	Yield (%)	HPLC Area % Purity
1	62	49	65	98.5
2	85	57	56	98.6
3	95	72	63	95.0

[a] Conditions: **1** (1 equiv), **2** (1.1 equiv), NaO*t*Bu (1.3 equiv), $Pd(OAc)_2$ (0.04 equiv), $PtBu_3.HBF_4$ (0.04 equiv), toluene (4 ml/g **1**), 95 °C, 4 h

2.2 Second Generation Development: Weak Base α-Arylation

Although the P*t*Bu$_3$·HBF$_4$/NaO*t*Bu process was implemented successfully on multi-kilo scale, we identified several issues that needed to be addressed in order to achieve a commercially viable α-arylation process. These issues included a) the instability of the product and starting material to the reaction conditions; b) the variability in impurity levels; c) the tedious and inconsistent alumina filtration; and d) the necessity of several different solvents which resulted in inefficient distillations.

The root of all concerns discussed above was the use of a strong base NaO*t*Bu. Hence, we refocused our efforts toward using weaker bases. We postulated that the use of weakly basic conditions would result in better stability of **1** and **3**, resulting in improved impurity profile, reduced level of colored impurities and thus avoid the need for an alumina filtration. We were also determined to find a catalyst/ligand system that would

minimize the formation of impurity **6**. Our optimization efforts included a broader number of solvents compared to our earlier work and utilized the preformed Pd(0) catalyst, Pd(P*t*Bu$_3$)$_2$ to reduce issues of active catalyst generation. Table 4 illustrates a subset of the bases and solvents included in the screen. It is important to note that polar aprotic solvents such as DMF, NMP or DMSO were detrimental to the reaction. Notably, the best combinations of conversion and yield were observed when using *t*-amyl alcohol in combination with several bases. The optimal base/solvent combination for the reaction was found to be K_3PO_4 in *t*-amyl alcohol.

Table 4: Second Generation Base/Solvent Optimization for α-Arylation Reaction[a]

Entry	Base	Solvent	Conversion (%)[b]	Product (%)
1	K_2CO_3	Toluene	0	0
2	K_2CO_3	MeTHF	0	0
3	K_2CO_3	*t*-Amyl OH	14	12
4	Cs_2CO_3	Toluene	11	9
5	Cs_2CO_3	MeTHF	8	7
6	Cs_2CO_3	*t*-Amyl OH	7	6
7	Na_3PO_4	*t*-Amyl OH	0	0
8	K_3PO_4	Toluene	13	11
9	K_3PO_4	MeTHF	22	18
10	K_3PO_4	*t*-Amyl OH	72	58

[a] Conditions: **1** (1 equiv), **2** (1.1 equiv), base (3 equiv), Pd(P*t*Bu$_3$)$_2$ (0.04 equiv), solvent (10 ml/g **1**), 80 °C.

[b] Conversion based on HPLC Area Percent of Product and Starting material

With optimal base and solvent conditions in hand we focused on improving the catalyst for this transformation. The initial optimization employed [(allyl)PdCl]$_2$ in combination with several ligands. Representative results are shown in Table 5. We observed that bidendate ligands (Xantphos, DPE-Phos) generally were not effective, providing approximately 30% conversion. When using catalysts derived from monodentate ligands, we observed that simple trialkylphosphines possessing a large cone angle (P*t*Bu$_3$) promoted the desired arylation reaction; whereas smaller trialkyl phosphine

derived catalysts (PCy_3) led to minimal conversion. Based on these findings, we systematically studied the effect of a variety of bulky, biaryl phosphine ligands on the reaction. Biaryl phosphines containing cyclohexyl groups on the phosphine center were found to give significantly higher yields than biaryl phosphines containing *tert*-butyl or aryl groups. Furthermore, the presence of a coordinating functional group (OMe, O*i*Pr) on either ring of the biaryl system led to improved conversion and yield (Table 6).

Table 5: Ligand Screening Results[a]

Entry	Ligand	Conversion (%)[b]	Cone Angle	Product (%)
1	$P(tBu)_2Me \cdot HBF_4$	0	161[14]	0
2	$PCy_3 \cdot HBF_4$	0	170[15]	0
3	$PtBu_3 \cdot HBF_4$	45	182[8]	34
4	$P(Ad)_2nBu$	7	ND	2
5	DPE Phos	34	N/A	30
6	XantPhos	30	N/A	24

[a] Conditions: **1** (1 equiv), **2** (1.1 equiv), base (3 equiv), $[(Allyl)PdCl]_2$ (0.0125 equiv), Ligand (0.05 equiv), *t*-amyl alcohol (10 ml/g **1**), 90 °C.

[b] Conversion based on HPLC Area Percent of product and starting material

Table 6:Effect of Substituted Biaryl Phosphines on Reaction Conversion[a]

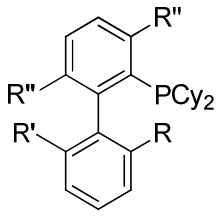

Entry	Ligand	R	R'	R''	Conversion (%)[b]	Product (%)	Product/ Conversion
1	$PtBu_3 \cdot HBF_4$	N/A	N/A	N/A	45	34	0.76
2	John Phos	H	H	H	25	5	0.20

3	MePhos	Me	H	H	28	12	0.42
4	X-Phos	iPr	iPr	H	66	52	0.79
5	Dave Phos	NMe_2	H	H	72	54	0.75
6	S Phos	OMe	OMe	H	76	65	0.86
7	RuPhos	OiPr	OiPr	H	96	90	0.94
8	Brett Phos	iPr	iPr	OMe	98	93	0.95

[a] Conditions: **1** (1 equiv), **2** (1.1 equiv), base (3 equiv), $[(Allyl)PdCl]_2$ (0.0125 equiv), Ligand (0.05 equiv), *t*-amyl alcohol (10 mL/g **1**), 80 °C.

[b] Conversion based on HPLC Area Percent of product and starting material

Based on the performance of X-Phos, RuPhos and S-Phos compared to other biaryl phosphines, we drew several conclusions with respect to ligand structure and reaction performance. First, 2,6-disubstitution on the bottom aromatic ring leads to better in process purity and improved conversion. Second, the presence of a coordinating substituent on the upper aromatic ring led to significant improvements in the reaction impurity profile and conversion. For example, superior reactivity was observed with BrettPhos.

After screening various Pd(II) and Pd(0) precursors, we selected the following experimental conditions: $Pd(OAc)_2$, BrettPhos, and K_3PO_4 in *t*-amyl alcohol. Unfortunately, we could not obtain sufficient amounts of Brett Phos to satisfy our campaign needs, while adequate quantities of RuPhos were available within our project timelines. Using RuPhos in place of BrettPhos resulted in modest reduction of solution yields (90% vs 95%) and required higher catalyst loading (2.5 mol% vs. 1.5 mol%) to achieve similar reaction kinetics (Figure 5). After surveying a broad range of reaction parameters using the $Pd(OAc)_2$/RuPhos conditions, we found that several variables directly impacted the rate and impurity profile of the reaction (Table 7). Specifically, increasing the base stoichiometry (entry 1 vs. entry 2), minimizing base particle size (entry 1 vs entry 6), minimizing reaction water content (entry 4 vs entry 5), and increasing temperature (entry 2 vs 3) accelerated the reaction rate while maintaining a consistent impurity profile. Notably, prolonged reaction times led to inferior impurity profile (entry 4). Based on these studies we obtained the following optimal conditions:

2.5 mol% $Pd(OAc)_2$, 5.0 mol% RuPhos, 4.0 equiv K_3PO_4 in *t*-amyl alcohol (4 L/kg **1**) at 95 °C. Under these reaction conditions, product **3** was obtained in 90% solution yield.

Figure 5: Reaction Profile of α-Arylation Reaction Using $Pd(OAc)_2$/BrettPhos and $Pd(OAc)_2$/RuPhos

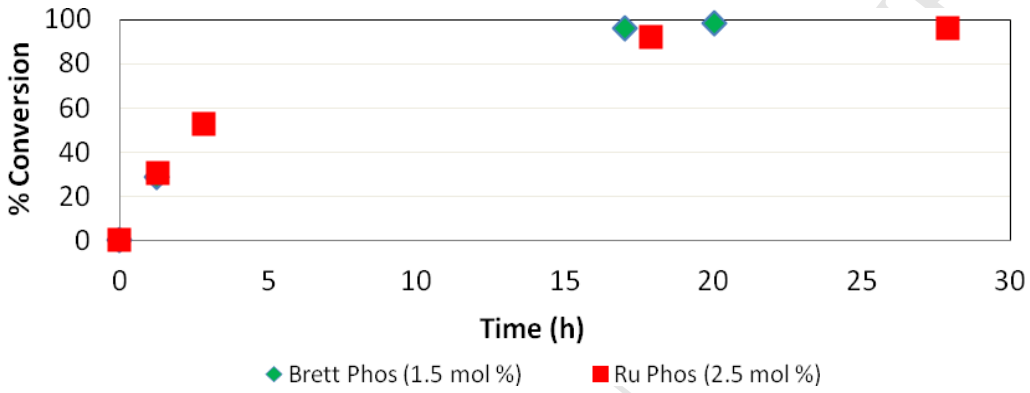

Table 7: Optimization Studies Using $Pd(OAc)_2$/RuPhos/K_3PO_4 in t-Amyl Alcohol[a]

Entry	Base Equiv	Base Particle Size (in)	Temperature (°C)	Water Content (equiv)	Time (h)[b]	Product (%)
1	4	0.025	85	0	16	94
2	6	0.025	85	0	12	93
3	4	0.025	105	0.4	9	92
4	4	0.075	85	0.4	34	89
5	4	0.075	85	0	19	93

[a] Reaction carried out using **1** (1 equiv), **2** (1.2 equiv), $Pd(OAc)_2$ (0.025 equiv), RuPhos (0.05 equiv), *t*-amyl alcohol (4 mL/g **1**)

[b] Reaction time represents time required to reach 98% conversion

A key concern throughout this development work was the heterogenous nature of the reaction. Employing an insoluble base, such as K_3PO_4, in large scale reactions using over head stirring can often be problematic, leading to variable reaction rates and

potential reaction stalling. In these systems, the only base available to the reactants is on the surface of the base particle. Therefore, understanding base particle size and maximization of available base surface area is extremely important for achieving consistent reaction performance. Our initial analysis indicated that minimization of base particle size increased the base surface area and increased the reaction rate. A complicating factor in this analysis was the water content of the reaction mixture, which caused the solid base to agglomerate, increasing base particle size, and slowing the reaction rate. Carrying out the reaction using K_3PO_4 of various particle sizes and water content (KF, Karl Fischer) showed that in order to obtain full conversion in less than 15 hours, we needed to control the base particle size to less than 400 µm and base water content to <3.0 wt% (Figure 6). Additional studies comparing base particle size to agitation rate indicated that controlling base particle size to less than 400 µm is optimal to achieve maximum base suspension under normal agitation conditions.

Figure 6: Effect of Potassium Phosphate Particle Size and KF on Reaction Rate

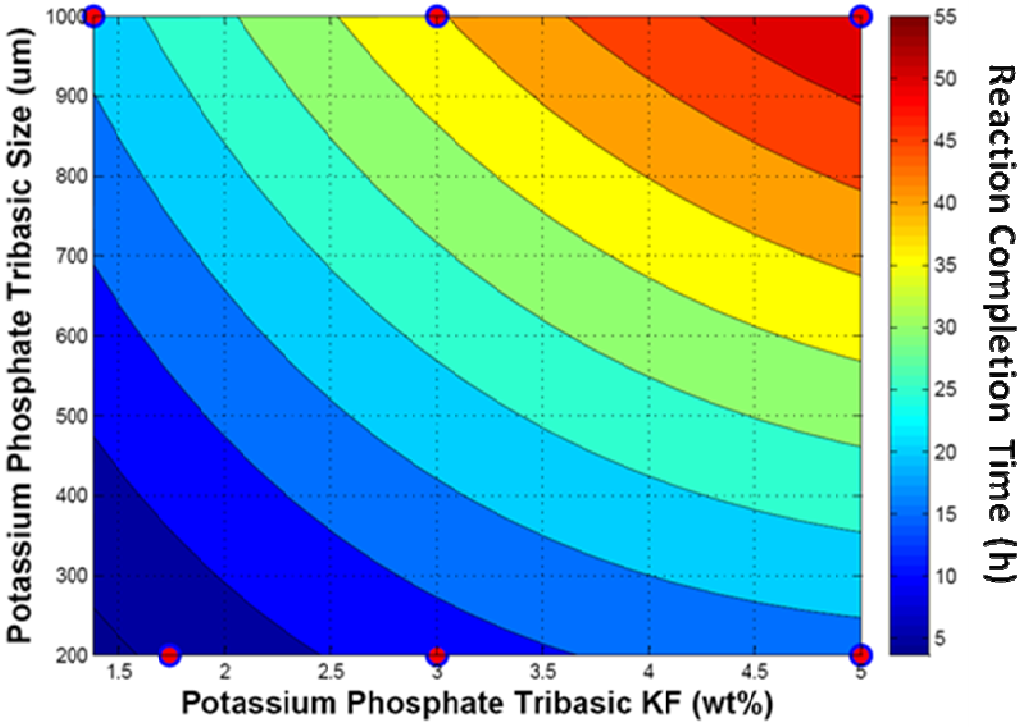

Using these reaction conditions, we observed impurities **5**, **7** and **8** (Figure 4), but notably, impurity **6** was not formed. Impurities **7** (α-hydroxylation) and **8** (rearrangement) can be controlled to <2 % by controlling headspace oxygen content to below 0.5 % during the reaction. Impurity **5** is controlled to less than 2 % by using fewer equivalents of base and maintaining the reaction temperature below 100 °C. In addition to these impurities, we also observed the ligand-related impurities RuPhos and RuPhos oxide. Notably, we were also able to detect the oxidative addition complex **9** (Figure 7) by HPLC and tentatively characterized **9** by HPLC-MS, providing us with a reliable method to confirm active catalyst formation. We were also able to confirm complex **9** by an independent synthesis of [(Ruphos)PdAr(Br)] from Pd_2dba_3 and Ruphos.

Figure 7: Oxidative Addition Complex 9 Formed in the α-Arylation Reaction

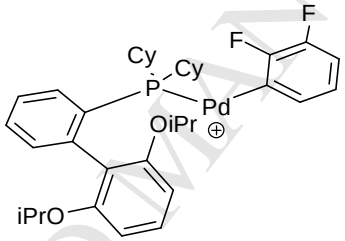

(**9**)

NB: Cationic complex **9** has been characterized by LCMS and MS/MS.

Our next challenge was to develop an isolation protocol that provided high quality product directly from the crude reaction mixture, eliminating the need for time consuming distillations and solvent exchanges. Our optimized conditions to remove K_3PO_4 employed the addition of 1 M HCl to the reaction mixture to dissolve the residual base and acidify the stream, resulting in rapid and clean phase splits. Due to the high solubility of the product in a wide range of organic solvents such as heptane, the only viable antisolvent for the crystallization was water. Unfortunately, the immiscibility of *t*-amyl alcohol and water required the use of a water miscible co-solvent in this crystallization. After screening several co-solvents in different ratios we found we found 1:2:2.5 of t-amyl alcohol:IPA:water (v/v/v) was the optimal ratio for the ternary solvent crystallization.

Removal of the oxidative addition complex **9**, which persisted during the crystallization, was challenging and led to higher palladium levels in the isolated material. There was a strong correlation between pH of the mother liquor and the palladium content in the isolated material (Table 8). As a result, we reasoned that we might be able to change the nature of complex **9** by manipulating the pH, for example, by protonating the ligand in an acidic media. Indeed, as we lowered the pH of the stream to <0.7, we obtained lower levels of palladium in the isolated cake (entries 1 and 2, Table 8). At lower pH, however, we started to observe desilylation of the product. Although this procedure provided a path forward to generate material of the desired color and quality, we felt it would be difficult to consistently achieve a mother liquor pH of <0.7 while maintaining product stability.

Table 8: Effect of pH on Product Quality and Appearance

Entry	pH	% loss ML	% loss wash	Isolated yield %	Potency %	HPLC Area % Purity	Pd (ppm)
1	0.43	15%	3%	76%	100.0%	100.0%	98
2	0.69	13%	4%	78%	99.0%	100.0%	440
3	1.3	11%	2%	80%	96.6%	100.0%	760
4	1.64	11%	2%	82%	95.7%	99.8%	1200

In order to develop a more robust isolation process, we developed a strategy to degrade and remove complex **9**. We found that treatment of the HCl washed reaction stream with aqueous cysteine (0.5 wt%) at 50 °C led to complete decomposition of complex **9** over the course of 4 hours, resulting in the formation of a proposed "Pd-cysteine" complex **10** and RuPhos (Figure 8). The decomposition of complex **9** could be clearly monitored by HPLC due to its UV absorbance. After removal of the lean aqueous phase, **3** could be crystallized, using the aforementioned *t*-amyl alcohol/IPA/water, as an off-white solid. Unfortunately, the isolated material was contaminated with residual RuPhos, which crystallizes readily under these conditions. Our strategy to remediate RuPhos from isolated **3** was based upon the basicity of this ligand, which has a p*K*a of

7.1, and the pH effect observed earlier (Table 8). Based on this data, we determined that acidification of the crystallization medium to a pH of ≤4 should lead to protonation of the ligand rendering it soluble in the partially aqueous mother liquor and product desilylation was not an issue at this pH range. Therefore, we modified the crystallization conditions to employ a 1:2:2.5 volume ratio of *t*-amyl alcohol:IPA: aq. H_3PO_4 (0.25 M), resulting in complete removal of RuPhos from isolated **3**. The optimized crystallization conditions were employed on 700 g scale to provide **3** in 73 M% isolated yield in high quality (99.8 HPLC Area % purity, 97 wt% potency).

Figure 8: Decomposition of Oxidative Addition Complex 9 with Cysteine

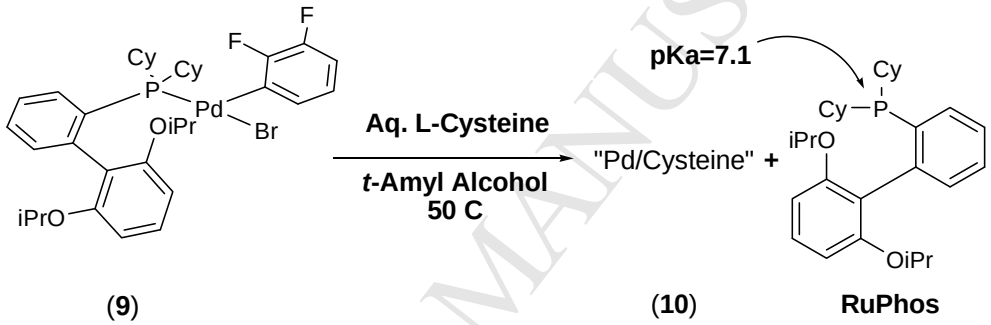

(**9**) (**10**) **RuPhos**

Table 9: Comparison of the First and Second Generation α-Arylation Processes

Process	Reaction Yield %	Isolated Yield %	HPLC Area % Purity	# Unit Operations
NaO*t*Bu/P*t*Bu$_3$.HBF$_4$	80%	61%	97.4%	7
K_3PO_4/RuPhos	90%	73%	99.8%	4

4. Conclusion

Two processes for the α-arylation reaction between cycloheptyl pyridyl ketone **1** and difluorobromo benzene **2** were described. The first generation process utilized $Pd(OAc)_2$/P*t*Bu$_3$.HBF$_4$ catalyst system with a strong base NaO*t*Bu. Although this process was demonstrated on multi-kilo scale it suffered from several operational, quality and throughput issues. As a result a second generation process was developed using a $Pd(OAc)_2$/RuPhos catalyst system with the weaker base K_3PO_4 in t-amyl alcohol. This

new weak base process was superior in several respects compared to the strong base process. As presented in Table 9, the new conditions afford higher yield, improved quality of product and reduced the number of unit operations. To the best of our knowledge, this is the first example of the use of $Pd(OAc)_2$/RuPhos/K_3PO_4 in *t*-amyl alcohol for an α-arylation reaction on scale. In order to scale the palladium catalyzed α-arylation reaction we addressed several important process considerations: a) catalyst generation and stability; b) base particle size; c) stability of starting material and product under the reaction conditions; d) moisture and oxygen content; e) understanding impurity origin and fate and f) removal of palladium species and impurities. By acquiring detailed knowledge around each of the process considerations, we were able to design an efficient and scalable α-arylation process.

5. Acknowledgements

The authors wish to acknowledge David Kronenthal, Susanne Kiau, Martin Eastgate, Francisco Gonzalez Bobes and Rajendra Deshpande for reviewing the paper and helpful discussions. The authors also want to acknowledge Charles Pathirana, Michael Peddicord, Wei Ding, Jonathan Marshall, Frank Rinaldi, and Merrill Davies for impurity characterization and analytical support. Additionally Victor Rosso, Jose Tabora, Xinhua Qian, Renee Randazzo, Vidya Iyer, and Alan Braem are acknowledged for experimental design and campaign support.

6. Experimental

a. Instrumentation

NMR spectra were obtained on a Bruker 400 (399.96 MHz for ^1H; 100.57 MHz for ^{13}C) spectrometer. ^1H NMR chemical shifts are reported in parts per million (ppm) relative to TMS, with the residual solvent peak used as an internal reference. Multiplicities are reported as follows: singlet (s), doublet (d), doublet of doublets (dd), triplet of doublets (td), triplet (t), multiplet (m), and broad resonance (br).

b. Procedure and Characterization

(6*S*,9*R*)-6-(2,3-difluorophenyl)-9-((triisopropylsilyl)oxy)-6,7,8,9-tetrahydro-Hcyclohepta[b]pyridin-5-one (**3**)

First Generation Strong Base Process:

A mixture of toluene (14.9 L), **2** (3.50 kg, 18.1 mol), **1** (4.92 kg, 14.8 mol), palladium acetate (0.132 kg, 0.588 mol), tri-tertbutylphosphonium tetrafluoroborate (0.174 kg, 0.600 mol), and sodium *tert*-butoxide (1.88 kg, 19.6 mol) was heated to 95 °C for 4 h. The resulting dark mixture was cooled to 25 °C and diluted with ethyl acetate (44.5 L), washed with saturated ammonium chloride solution (2x24.7 L), phase split and concentrated the organic to ~ 25 L under vacuum. The dark solution was absorbed onto a packed bed of alumina (19.8 kg) and eluted with toluene (203 L). The fractions containing **3** were combined and solvent swapped to IPA and concentration to 3 L/Kg of **3**. The IPA solution brought to 45 °C and Water (1.5 L/Kg) was added to the solution over 10 min, and the mixture seeded with 5 wt% **3**. The mixture was cooled to 40 °C over 2.5 h and Water (1.5 L/Kg) was added to the solution over 50 min. The resulting slurry was cooled to 25 °C over 1 h and aged for an additional 1 h followed by filtration. The cake was washed with a solution of IPA/water (1:1, 9.17 L) and dried under vacuum (at atmospheric pressure, 50 °C) for 24 h to afford **3** (4.15 kg, 63 %, 12:1 dr). [α] 20 D +166.7 (c 3.12, MeOH); Mp = 93.5-94.2 °C; ^{1}H NMR (400 MHz, DMSO d-6) δ 8.66 (dd, *J* = 4.8, 1.8 Hz, 1H), 7.91 (dd, *J* = 7.7, 1.7 Hz, 1H), 7.53 (dd, *J* = 7.7, 5.0 Hz, 1H), 7.36-7.29 (m, 1H), 7.20-7.14 (m, 1H), 7.04-7.01 (m, 1H), 5.22(dd, *J* = 4.0, 2.0 Hz, 1H), 4.65 (dd, *J* = 12.3, 2.2 Hz, 1H), 2.29-2.21 (m, 2H), 2.10-2.02 (m, 1H), 1.99-1.93 (m, 1H), 1.04-0.95 (m, 3H), 0.92 (d, *J* = 7.1 Hz, 9H), 0.86 (d, *J* = 7.1 Hz, 9H); ^{13}C NMR (125 MHz, DMSO d-6) δ 204.4, 160.4, 159.4, 150.9, 149.8 (dd, *J* = 245.2, 13.2 Hz), 147.6 (dd, *J* = 244.4, 12.4 Hz), 137.1, 132.8, 132.7 (d, *J* = 12.4 Hz), 125.0, 123.8, 115.8 (d, *J* = 16.8), 76.2, 49.0, 32.6, 26.7, 17.6, 11.4; ^{19}F NMR (376 MHz, DMSO d-6) δ -139.1 (ddd, *J* = 21.8, 10.3, 5.7 Hz), -142.4 (d, *J* = 20.7 Hz); IR (KBr) 3444 (br), 2943, 2866, 1689, 1488, 1264, 1083 cm^{-1}; HRMS Calcd for $C_{25}H_{34}F_2NO_2Si$: 446.2321; HRMS found [M + H]+: 446.2317.

Second Generation Weak Base Process:

A 10 L reactor equipped with an overhead stirrer was charged with **1** (0.63 kg, 1.89 mol), *t*-amyl alcohol (2.5 L), potassium phosphate tribasic (1.63 kg, 7.56 mol), palladium acetate (10.43 g, 0.046 mol), RuPhos (43.36 g, 0.092 mol), and **2** (0.43 kg, 2.23 mol)

under a nitrogen atmosphere. The resulting suspension was heated to 95 °C until < 2 % of **1** remained as judged by HPLC analysis. The mixture was cooled to 15 °C followed by slow addition of aq. HCl (5.7 L, 1 M) to the mixture while maintaining the batch temperature below 30 °C. The resulting biphasic mixture was agitated for 15 min at 25 °C . Agitation was stopped and the lower aqueous layer was removed. The rich organic phase was diluted with *t*-amyl alcohol (1.4 L) and treated with an aqueous solution of L-cysteine (5.50 L, 5 wt %). The resulting biphasic mixture was heated to 50 °C for 2 h followed by cooling to 25 °C. Agitation was stopped and the lower aqueous layer was removed and the rich organic phase was polish filtered thru a 1 υm line. The rich organic filtrate was concentrated to 3 L/kg **1** via vacuum distillation (75 torr, 50 °C batch temperature) followed by dilution with isopropanol (0.7 L). The distillation was continued with constant addition of isopropanol until the ratio of isopropanol:*t*-amyl alcohol >75:25 % v/v as judged by GC analysis. The batch was returned to atmospheric pressure and heated to 40–45 °C. Aq. H_3PO_4 (0.7 L) was slowly added to the mixture while maintaining the batch temperature >40 °C followed by the addition of seeds of **3** (7 g, 1 wt %). The resulting slurry was aged at 40 °C for 1 h. Aq. H_3PO_4 (1.1 L) was slowly added to the batch while maintaining the batch temperature > 40 °C. The slurry was held for 1 h at 40 °C, followed by cooling to 0 °C over 6 h. The slurry was isolated by filtration. The wet cake was washed with 47/35/18 %v/v aq. H_3PO_4/isopropanol/*t*-amyl alcohol (1x2.1 L), 50/50 %v/v isopropanol/water and dried (50 °C/100 torr) to provide **3** (0.60 kg, 73 %) as an off-white solid.

7. References and Notes

[1] a) Goadsby, P. J. *Drugs* **2005**, *65*, 2557. (b) Bell, I. M.; Bednar, R. A.; Fay, J. F.; Gallicchio, S. N.; Hochman, J. H.; McMasters, D. R.; Miller-Stein, C.; Moore, E. L.; Mosser, S. D.; Pudvah, N. T.; Quigley, A. G.; Salvatore, C. A.; Stump, C. A.; Theberge, C. R.;Wong, B. K.; Zartman, C. B.; Zhang, X.-F.; Kane, S. A.; Graham, S. L.; Vacca, J. P.; Williams, T. M. Bioorg. Med. *Chem. Lett.* **2006**, *16*, 6165. (c) Goadsby, P. J.; Lipton, R. B.; Ferrari, M. D. N. *Eng. J. Med*. **2002**, *346*, 257. (d) Olesen, J.; Diener, H. C.;

Husstedt, I.W.; Goadsby, P. J.; Hall, D.; Meier, U.; Pollentier, S.; Lesko, L. M. N. *Eng. J. Med.* **2004**, *350*, 1104

[2] Luo, G.; Chen, L.; Conway, C. M.; Denton, R.; Keavy, D.; Gulianello, M.; Huang, Y.; Kostich, W.; Lentz, K. A.; Mercer, S. E.; Schartman, R.; Signor, L.; Browning, M.; Macor, J. E.; Dubowchik, G. M. *ACS Med. Chem. Lett*. **2012**, *3*, 337 and references therein.

[3] Leahy, D.K.; Fan, Y.; Desai, L.V.; Chan, C.; Zhu, J.; Luo, G.; Chen, L.; Hanson, R.L.; Sugiyama, M.; Rosner, T.; Cuniere, N.; Guo, Z.; Hsiao, Y.; Gao, Q, *Org. Lett.*, **2012**, *14*, 4938.

[4] Culkin, D. A.; Hartwig, J. F. *Acc. Chem. Res.* **2003**, *36*, 234.

[5] a) Satoh, T.; Kawamura, Y.; Miura, M.; Nomura, M. *Angew. Chem., Int. Ed. Engl.* **1997**, *36*, 1740.; b) Miura, M.; Nomura, M. *Top. Curr. Chem.* **2002**, *219*, 211. c) Y.; Satoh, T.; Miura, M.; Nomura, M *Tetrahedron Lett.* **2002**, *43*, 101.; d) Miura, M.; Satoh, T. *Palladium in Organic Synthesis*; Springer: Berlin/ Heidelberg, 2005; Vol. 14. e) Terao, Y.; Fukuoka, Y.; Satoh, T.; Miura, M.; Nomura, M *Tetrahedron Lett.* **2002**, *43*, 101.

[6] a) Palucki, M.; Buchwald, S. L. *J. Am. Chem. Soc.* **1997**, *119*, 11108.; b) Moradi, W. A.; Buchwald, S. L. *J. Am. Chem. Soc.* **2001**, *123*, 7996.; c) Martín, R.; Buchwald, S. L. *Angew. Chem., Int. Ed.* **2007**, *46*, 7236

[7] a) Hamann, B. C.; Hartwig, J. F. *J. Am. Chem. Soc.* **1997**, *119*, 12382.; b) Hama, T.; Liu, X.; Culkin, D.; Hartwig, J. F. *J. Am. Chem. Soc.* **2003**, *125*, 11176.; c) Liu, X.; Hartwig, J. F. *J. Am. Chem. Soc.* **2004**, *126*, 5182.; d) Vo, G. D.; Hartwig, J. F. *Angew. Chem., Int. Ed.* **2008**, *47*, 2127

[8] a) Bellina, F.; Rossi, R. *Chem. Rev*. **2010**, *110*, 1082; b) Burtoloso, A. C. B. *Synlett* **2009**, 320; c) Lloyd-Jones, G. C. *Angew. Chem. Int. Ed*. **2002**, *41*, 953

[9] Desai, L.V.; Ren, D.T.; Rosner, T, *Org. Lett.*, **2010**, *12*, 1032

[10] Although these conditions were attractive due to the unprecedented application of CxPOMeCy ligand in an α-arylation reaction, we ran into several impurity and palladium removal issues during isolation upon scale-up

[11] All impurities were characterized and their structures predicted based on chemical formulas and fragmentation pattern obtained by MS/MS and LCMS.

[12] Lyons, T. W.; Sanford, M. S., *Chem. Rev*., **2010**, *110*, 1147 and references therein.

[13] Hartwig has proposed a mono-ligated complex to be the catalytic active species for arylation of esters with arylbromides when using $PtBu_3$ ligand with NaOtBu. Hama, T.; Hartwig, J. F.; *Org. Lett*. **2008**, *10*, 1545

[14] Rahman, M. M.; Liu, H. Y.; Prock, A.; Giering, W. P. *Organometallics* **1987**, *6*, 650

[15] Tolman, C. A. *Chem. Re*v. **1977**, *77*, 313